An *in Vitro* Evaluation of the Biological Activity of Biogenic Eggshell Derived Nano-Sized Bioglass, Poly (ε-Caprolactone), and Zein Protein 3D Composite Scaffolds for Bone Tissue Engineering

Amany Sabry El-Korashy[1*], El-Shahidy, M.S.[2], Rania El-Saady Badawy[1], Nour Ahmed Habib[3]

[1]Department of Dental Biomaterials, Faculty of Dentistry, Suez Canal University, Ismailia, Egypt
[2] Department of Virology, Faculty of Veterinary Medicine, Suez Canal University, Ismailia, Egypt
[3] Department of Dental Biomaterials, Faculty of Dentistry, Cairo University, Egypt

ABSTRACT

Applying biologically active scaffolds to promote bone tissue regeneration and reduce environmental pollution caused by biological waste are the main goals of this study. Sol-gel methods were utilized in this study to create nano-sized bioactive glass ceramics, which are frequently used as graft material or bone filler. Two synthesis routes were compared: one utilizing pure chemicals and the other utilizing biogenic $CaCO_3$ sourced from eggshell waste as an innovative approach. X-ray diffraction and Fourier transform infrared analyses showed that both bioglass powders consisted of amorphous phases with particle sizes of crystals measuring 14–16 nm, as observed through transmission electron microscopy. Upon immersion in phosphate-buffered saline, carbonate apatite crystals were observed to develop on the surfaces of solid bioglass and composite polymeric scaffolds composed of polycaprolactone/zein protein. These porous and non-toxic scaffolds facilitated osteoblast attachment, proliferation, and differentiation. The incorporation of bioglass enhanced mechanical properties, rates of biodegradation, and cell behavior. Incorporating biogenic bioglass powder into the PCL/Zein scaffold matrix improved the thermal stability of the synthesized scaffolds. Biogenic bioglass contributed to the bioactivity, degradation rate, viability, and calcium deposition of bone marrow Mesenchymal stem cells (r-BMMSC) to a certain extent. This study explores the utilization of eggshell waste as a cost-effective source of calcium for Nano-bioglass synthesis. The resulting nano-bioglass was incorporated into 3D PCL/Zein composite scaffolds for bone tissue engineering in non-load-bearing areas. Furthermore, the study suggests the application of biogenic bioglass in dentistry for oral care product fabrication due to its superior bioactivity compared to chemically synthesized bioglass.

Keywords: Biogenic bioglass; Bone tissue engineering; Eggshell waste; Polycaprolactone; Scaffolds; Sol-gel synthesis; Zein protein.

INTRODUCTION

Every year, thousands of medical procedures are completed to fix or replace damaged human tissues. Auto grafts, allografts, and xenografts are different techniques to replace damaged tissues. There are a few things to think about when using these methods. Some of its problems include a lack of donors or donor sites, the spread of disease, graft rejection, pain, and death at the donor site. To overcome the drawbacks of these traditional treatments, tissue engineering has emerged as a rapidly evolving method of rebuilding damaged tissues rather than replacing them (Qi *et al*., 2021). A three-dimensional porous bioresorbable scaffold acts as a template to facilitate initial cell attachment, followed by tissue formation in vivo and in vitro. Characteristic criteria of ideal scaffolds include appropriate porosity and pore size, enhanced cell ingrowth, enough mechanical strength, adequate degradation properties, and biocompatibility. Due to the inability of any individual material to fulfill all of these criteria, composite structures that integrate the benefits of many materials are considered more favorable.

The combination of polymers and bio-ceramic fillers allows for the utilization of polymer shaping techniques while benefiting from the enhanced strength, rigidity, and bioactivity provided by the bio ceramic fillers. This results in improved physical, mechanical, and biological performance. Scientists have used several materials, such as metals, polymers (natural or synthetic), ceramics, and their composites, as scaffolds for tissue engineering. Although natural polymers such as gelatin, collagen, starch, fibrinogen, cellulose, chitin, zein, etc., are biocompatible and closely mimic the natural extracellular matrix (ECM) of tissues, their poor mechanical properties, high cost, uncontrollable degradation rate, and susceptibility to immunogenic reactions are limitations of their usage (Hamza *et al*., 2015).

Synthetic polymers, in contrast, can be customized to meet specific requirements, typically demonstrating consistent and foreseeable physical and mechanical characteristics, thus finding extensive application in biomedical fields. Polyesters such as polycaprolactone (PCL), polylactic acid (PLA), and polyglycolic acid (PGA) are prominent examples of synthetic polymers frequently employed in tissue engineering endeavors.

Polycaprolactone (PCL) is biodegradable aliphatic polyester that can be molded into different shapes. Besides being FDA-approved, PCL has excellent properties of thermal stability, easy processing, hydrophobicity, and degradation that can be greatly

_____

* *Corresponding author e-mail:* *amanysabryelkorashy@gmail.com*

altered through surface modifications. As a result of the intrinsic hydrophobic surface properties of PCL, its degradation is slowed down, and bone apposition or bonding on the polymer surface is restricted. This makes the material unfavorable for cell growth (Wu *et al*., 2012), finally limiting its use in tissue engineering. In order to address the challenges associated with utilizing an individual polymer, PCL should be used as a copolymer with a variety of synthetic or natural polymers, as well as bio-ceramics. Zein biopolymer, a major protein extracted from corn plants, is insoluble in water but soluble in ethyl alcohol solutions, with a promising potential for drug delivery and tissue engineering applications (Pérez-Guzmán and Castro-Muñoz, 2020).

Bioactive glasses are among the bio ceramic materials that act as bone substitutes and tissue regeneration matrices by reacting with the physiological fluids to form tenacious bonds to hard tissues through their cellular activity. These bio-glasses are prepared from pure chemical reagents using different techniques. More recently, some bio ceramic materials have been prepared from natural sources of biogenic waste materials, such as bovine bone, eggshells, and seashells (Mohd Pu'ad *et al*., 2019). Eggshell, as a bio-waste material, is a rich source of $CaCO_3$, exceeding 94% (Azis *et al*., 2018), showing various advantages of using biogenic eggshell waste as a calcium source for active Nano sized bioglass.

Eggshells represent a common waste product generated in daily activities, characterized by low costs and a wide array of raw material resources. Through the utilization of such waste material, there is potential for reducing environmental pollution, while elements such as Mg^{2+}, P^{5+}, Si^{4+}, and other trace elements beneficial for bone formation (e.g., strontium-substituted hydroxyapatite derived from eggshells) exhibit enhanced biological properties (Geng *et al*., 2018). Consequently, in this investigation, the sol-gel chemistry approach was employed to fabricate two solid materials using nano-sized 45S5 bio-glass (B.G) powder. Both solid materials share identical chemical compositions but diverge in terms of their precursor origins. The first solid was synthesized using conventional chemical reagents, while the second bioglass (B.G.) was derived from biogenic calcined eggshells, serving as a source of calcium oxide. This innovative approach utilizing eggshells as a raw material for bio ceramic production within a polymeric matrix for tissue regeneration represents a novel application in the field. Subsequently, each variant of the synthesized bioglass was individually incorporated into polycaprolactone/zein scaffold matrices to fabricate 3D composite scaffolds intended for bone tissue engineering purposes.

In order to evaluate the impact of the bio-glass synthesis methods and their reactivity on the characteristics and functionality of the composite scaffolds, a series of *in vitro* assessments encompassing physical, mechanical, and biological analyses were conducted on the scaffolds.

MATERIALS AND METHODS

The current study obtained approval from the Research Ethics Committee at the Faculty of Dentistry, Suez Canal University, under Protocol Code No. 123/2018.

Synthesis of Nano-bioglass using pure chemical reagents

Nano-bioglass (n-BG) with the chemical composition CaO-SiO_2-Na_2O-P_2O_5 = 46.1–26.9–34.4–2.6 mole% is prepared in an inorganic chemistry laboratory by a quick alkali-mediated sol-gel method reported by Xia and Chang, (2007), with little modification. The used chemicals are Sigma-Aldrich Products (Germany), except the ammonia solution (BDH Annular, England). The following chemical materials are used in the preparation: calcium nitrate tetrahydrate (CNTH) $[Ca(NO_3)_2.4H_2O]$ (source of CaO), tetraethyl ortho silicates (TEOS) (source of SiO_2), sodium nitrate $NaNO_3$ (source of Na_2O), triethyl phosphate (TEP) (source of P_2O_5), and ammonia solution for adjusting the pH of the reaction (pH=10). Bioglass gels are prepared through a hydrolysis and polycondensation reaction between stoichiometric am-ounts of the bioglass ingredients.

For thirty minutes, precisely 9.8 ml of TOES, 2 ml of 2M HNO_3, and 50 ml of 70% ethyl alcohol are stirred in a 1000 ml conical flask equipped with a magnetic stirrer. Subsequently, 0.95 ml of TEP is added to the TOES solution and stirred for an additional 20 minutes. Simultaneously, 6.35 g of CNTH is combined with 120 ml of deionized water at ambient room temperature.

This mixture is stirred for 15 minutes and then added to the previous reaction mixture. The first mixture that had been dissolved in 50 ml of deionized water was then mixed with 4.14 g of $NaNO_3$ and stirred for another 10 minutes. 1 M of (NH_4OH) solution is added with vigorous stirring (until pH: 10), with the occurrence of a rapid gelation of the sol. The gel obtained was forcefully agitated, rinsed with distilled water, filtered, and subjected to a drying process at a temperature of 60°C in a drying oven for 24 hours. The dehydrated gel underwent a 2-hour calcination process at a temperature of 700 ^{o}C using a muffle furnace. Once the calcined BG powder had cooled to room temperature, it was meticulously pulverized and sifted.

Synthesis of nano-bioglass using biogenic eggshells

The schematic illustration of the biogenic bioglass synthesis is depicted in Figure (1). The methodology employed for the fabrication of biogenic bio-glass (B.G) from eggshells mirrors that utilized for synthesizing B.G from pure chemical reagents via the sol-gel process, with the distinction being the utilization of eggshell waste as the source of calcium oxide (CaO). Specifically, 20 g of eggshells underwent a cleaning process with acetone to eliminate organic residues, followed by rinsing with a small quantity of 70% ethyl alcohol, and ultimately drying at 80°C for duration of 2 hrs. The dried eggshells are pulverized into a small

particulate and subjected to calcination for 2 hours at a temperature of 1000 ºC, resulting in the production of a white powder of CaO. Exactly 3.76 g of CaO eggshell is dissolved in 1M HNO_3 and used to prepare the final nano-bioglass powder.

Characterization of the eggshell powder and the synthesized nano-bioglass powders

Thermogravimetric analysis (TGA)

The Thermogravimetric Analysis (TGA) method is utilized to evaluate the thermal stability of the biogenic eggshell and determine the proportion of volatile constituents through weight loss measurements. The analysis is carried out utilizing a TGA instrument (Shimadzu DTG-60H) with a heating rate of 10°C/min, starting at ambient room temperature and ramping up to a peak temperature of 1000°C.

Inductive coupled plasma atomic emission spectroscopy (ICP-AES)

The percentage level of trace metals in calcined eggshell powder is estimated using ICP-AESICP-AES (Ion Bench with Agilent 8800 ICP-MS). Eggshell powder, CaO (20 mg), is dissolved in 50 ml of a 1.0 M nitric acid solution (69% nitric acid, AnalaR NORMAPUR® analytical reagent).

X-Ray diffraction analysis (XRD)

The XRD technique (a Bruker (Germany) D8 Advance X-ray diffraction model with CuKα radiation (0.15418 nm), 40 K.V., and 25 mA) is used to detect the phase compositions of the eggshell powder and the synthesized Nano-bioglass powders. The diffraction patterns ranging from 5 to 55°C are recorded in continuous mode at 2°C/min.

Attenuated total reflection fourier transform infrared (ATR-FTIR)

The main constituent chemical functional groups and the type of bonding between the various atoms in the groups of Nano-bioglass powders are analyzed using the ATR-FTIR spectrometer technique (Brucker, Germany, Alpha-P) at 400-4000 cm⁻¹ at a scanning speed of 2 cm⁻¹.

Scanning electron microscope (SEM) and energy dispersive X-ray (EDX)

SEM is employed to examine the morphology and chemical composition of the bioglass. This is done by using a Quanta 250 FEG (Field Emission Gun) attached to an EDX unit with an accelerating voltage of 30 kV (FEI Company, Netherlands).

Transmittance Electron Microscopy (TEM)

The morphology and crystal size of bioglass powders are analysed using a computer-controlled, high-resolution TEM (JEM-HR-2100, Japan), working at an accelerating voltage of 200 kV.

Bioactivity test of the bioglass powders

The capability of a material to form bonds with living tissues, *in vitro*, is closely associated with its ability to develop an apatite layer that mimics natural bonds when immersed in Phosphate-Buffered Saline (PBS) and/or Simulated Body Fluid (SBF) solutions (Loh *et al.*, 2023; Varila *et al.*, 2012). In the context of in vitro bioglass evaluation, 1 g of each dry solid powder is immersed in 100 ml of PBS (pH:7.4) and maintained at 37±1°C for a duration of 14 days (Loh *et al.*, 2023). The PBS solutions are refreshed every three days during the testing period. Upon completion of the experiment, the samples are filtered, rinsed with a deionized water, and subsequently dried at 50°C for 24 hrs. The solids are then subjected to analysis through X-ray Diffraction (XRD), Fourier Transform Infrared Spectroscopy (FTIR), Scanning Electron Microscopy (SEM), and Energy-Dispersive X-ray Spectroscopy (EDX) to evaluate their bioactive properties.

Nano-BG/Polymer Composite Scaffolds Fabrication

The polymers employed in fabricating the 3D scaffolds include polycaprolactone (PCL) with a molecular weight range of 70,000-90,000 Da and Zein protein polymers procured from Sigma-Aldrich Company. Using the solvent casting/particle leaching technique (Diba *et al.*, 2011), three different scaffold groups are produced as follows: Group (I): PCL: Zein at ratio of 80:20 wt. (%); Group (II): PCL: Zein: BG (Pure chemically synthesized in ratio of 60:20:20 wt. (%) and Group (III): PCL: Zein: BG (Biogenically synthesized from eggshells at ratio of 60:20:20 wt. (%).

Under vigorous mechanical stirring for 2 hours, a 10% (w/v) PCL solution is prepared by dissolving the PCL pellets (6 g) in a dry chloroform solvent. This is followed by the gradual addition of zein protein (1.5 g) (group I) and 30 g of pore-forming particles of NaCl
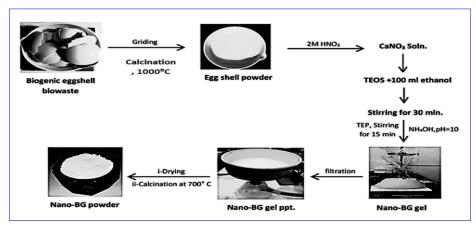

Figure (1): Schematic diagram of the main steps in the synthesis of nano-bioglass from biogenic eggshells.

(particle sizes 250–500 μm). For the synthesis of groups II and III, each type of bioglass (2 g) is added to the composite mixture before the addition of NaCl crystals. In all groups, the weight ratio of PCL to NaCl is 1:5, obtaining a homogeneous mix. A part of each composite mixture was placed directly into specialized disc-shaped Teflon molds with sizes of 8 x 3 mm and 10 x 20 mm. These molds are used to measure the mechanical strength and porosity of the scaffolds, respectively (Fig. 2).

For cell culture experiments and biodegradation testing, portions of each composite mixture were poured into a sterilized, dry, clean glass petri dish (35 mm internal diameter). All samples were kept at room temperature for 48 hrs to allow complete evaporation of the solvents and complete hardening of the composite scaffolds before being extracted from the molds. The extracted scaffolds are immersed in deionized water for 48 hours, being exchanged every 6 hours to help with the extraction of the NaCl crystals (porogen) from the scaffolds. The NaCl-free scaffolds are air-dried overnight, followed by drying in a vacuum drying oven (Model: DZF-6050, Germany) at 40 °C for 2 hrs.
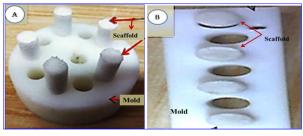

Figure (2): Measuring the mechanical strength (A) and porosity (B) of cylindrical composite scaffolds with dimension of 10 x 20 mm and 8 x 3 mm, respectively.

Composite Scaffolds Characterization

Physico-mechanical characterizations

In order to characterize the composite scaffold, six scaffold samples from each group (n = 6) were inspected for each test and thereafter put through an evaluation procedure.

Quantitative assessment of the porosity

The Ethyl alcohol displacement method (Zhang *et al.*, 2019) is used to assess the porosity of the scaffolds. Liquid of dry absolute ethyl alcohol is used since it does not react with PCL and/or zein protein.

Microstructure and Pore diameters

SEM is used to evaluate the microstructure and pore diameters of the composite scaffolds, which are divided into sections before examination using an extremely sharp metal stain-steel blade.

Compressive strength test

The compressive strength of scaffold groups, which have a length of 20 mm and a diameter of 10 mm, is evaluated using an Instron Universal Testing Machine. The specific machine used is the England-made frame model 3345, equipped with a load cell of 500 N and an N model of 2519-104).

In Vitro biodegradation test

Using a Fisher Scientific Electric Balance (USA), each sample is weighed to determine its initial dry wei-

ight (W_i), with values up to the fourth decimal number. The samples are immersed in PBS containing 0.02 wt. % sodium azide (NaN_3) to inhibit the bacterial growth and incubated at 37 ± 1 °C for 180 days. To ensure continuous ion activity and a stable environ-ment, the immersion solution is replaced every ten days. After the predetermined immersion periods, the samples are removed from the immersion solution, gently rinsed with distilled water, and dried at 40°C for 48 hrs. to determine their final weight, the dried samples are reweighed until a constant weight is achieved. The weight reduction percentage of each sample is calculated using the following equation:

$$L_{oss}\% = [(W_i - W_f) / W_i] \times 100$$

Where: L_{oss}, Weight loss percentage; W_i and W_f, initial dry weight and final weight at end period of the degradation, respectively.

In Vitro Scaffolds Bioactivity

The bioactivity of different composite scaffolds is evaluated by observing the formation of apatite crystals on their surfaces (Varila *et al.*, 2012). Each scaffold sample is immersed in 50 ml of PBS (pH: 7.4) for 14 days, kept at 37 ± 1°C for three days, with the solution being replaced every three days. Following the soaking period, the samples are gently rinsed with 15 ml of absolute ethyl alcohol, followed by 20 ml of deionized water, and then dried at 40°C for 24 hours. Surface morphology of the treated samples is examined using SEM and EDX.

Thermal Analysis and Evaluation (DTA and T.G) of the scaffolds

TGA and DTA are used to measure the mass loss and phase transitions of the scaffolds over a temp-erature range for groups (I) and (III), respectively. This is done to determine the effect of B.G. addition on the thermal stability of the scaffolds.

In Vitro cell-based assays

Isolation and Culture of Mesenchymal Stem Cells

Mesenchymal stem cells derived from a rat's femur bone marrow, specifically rBM-MSCs, are utilized to assess the ability of the produced polymeric scaffolds to promote cell adhesion and growth. These stem cells are sourced from the Central Lab for Stem Cell and Biomaterials Applied Research, situated in the Faculty of Dentistry at Ain Shams University. The isolation process and culture steps follow the protocols outlined by Sangeetha *et al.* (2017). Before conducting in vitro cell-based assays, the scaffolds undergo sterilization through two steps: immersion in absolute ethyl alcohol for 15 minutes and exposure to UV light for 20 minutes on each side.

Biological Evaluation Study

MTT (3-(4, 5-dimethyl thiazolyl-2)-2, 5-diphenyl-tetratetrazolium bromide assay

The MTT assay is utilized to assess the viability of cells adhered to and proliferating on the composite scaffolds. Sterilized scaffold sample discs were placed in a 96-well tissue culture plate and incubated for 24 hrs at 37°C with 5% CO_2. Subsequently, 1 x 10^5 cells/ml (100 μl/well) were added to each well

containing the scaffold. The inoculated samples were incubated for time interval 1, 3, and 7 days, respectively, under consistent condition using a Memmert 170 incubator (Schwa-Bach, Germany). After incubation, the samples were washed with phosphate-buffered saline (PBS) and transferred to new wells. Subsequently, 100 µl of a 5 mg/ml PBS solution was mixed with 200 µl of serum-free Dulbecco's Modified Eagle Medium (DMEM) containing 10% fetal bovine serum (FBS) and 50 mg/ml each of penicillin, streptomycin, and antifungal agents. The mixture was then agitated at 1500 rpm for 5 mins and incubated for 5 hrs to allow MTT metabolism. The remaining solution was aspirated, and 200 µl of Dimethyl sulfoxide (DMSO) was added to each well and vigorously mixed at 150 revolutions per minute for 5 min to ensure thorough dissolution of formazan in the solvent. The absorbance of the supernatant was measured at 570 nm using an ELISA reader (Mindray MR 96A, China) following the protocol outlined by Gautam *et a*l. (2021).

Alkaline phosphatase (ALP) activity assay

The ELISA approach is employed to facilitate the osteogenic proliferation of Mesenchymal stem cells derived from bone marrow on the scaffolds. The ALP activity is measured using an ALP Elisa Kit Assay (NOVA procedure, Cat. No. In-Hu0075) from the Doxing Industry Zone in Beijing, China.

Procedure

The scaffolds are subjected to the same steps applied in the MTT assay before seeding with rBM-MSCs. 1×10^5 third-passage rBM-MSCs are used to seed the samples. These are incubated at 37°C with 5% CO_2 under humidified conditions in osteogenic differentiation media for 1, 3, and 7 days, followed by washing with PBS and transferal to another 96-well plate. A buffer of 1 ml cell lysis (1 mM $MgCl_2$, 0.1 mM $ZnCl_2$, 20 mM TRIS buffered solution, and 0.1 wt. % Triton X-100) was added to each scaffold-containing well. The lysates are collected and centrifuged for 5 minutes at 2500 rpm (Hermle Labour Z 200A Universal Compact Centrifuge, Germany). 250 µl of the clear supernatant was incubated with 100 µl of ALP buffer solution, containing two mM MgCl, 9 mM p-NPP, and 0.1 mM Tris, in a new 96-well plate for about 60 minutes in a dark place at 37 ±0.5°C. 1 M NaOH (650 µl) was added to each well to stop the reaction. Sample absorbance is measured at 405 nm with an Elisa micro plate reader. Subsequently, a volume of 100 µl of ALP buffer was introduced to 250 µl of the transparent liquid remaining after centrifugation. The mixture was then subjected to incubation at a temperature of 37 ±0.5 °C for 5 minutes in an environment devoid of light. The ALP buffer solution is produced under the supervision of the Doxing Industry Zone in Beijing, China (NOVA protocol).

Evaluation of Calcium Deposit Formation Using Mineralization Assay (Alizarin Red S Staining)

The scaffolds are filled with rBM-MSCs and exposed to osteogenic differentiation medium at 37°C and 5% CO_2 for 3, 7 and 15 days. Following incubation, the cells undergo three gentle washes with PBS,

are then fixed in a 4% formaldehyde solution for 15 minutes at room temperature, and then washed three times with deionized water. The samples were treated with 1 ml of alizarin red and incubated for 20 minutes at room temperature with moderate agitation. The orange-red deposits on composite scaffolds and stained samples are examined using an inverted microscope (Leica Microsystems DMI80 inverted microscope platform and LAS X software, Germany). The samples were stored at -20 °C before dye extraction.

Quantification of the calcium deposition test

The cells are treated with 800 µl of 10% acetic acid for 30 minutes at room temperature with agitation. Subsequently, the cells are transferred to a 1.5-ml microcentrifuge tube containing 10% acetic acid, vigorously mixed for 30 seconds, covered with 500 µl of mineral oil, heated at 85°C for 10 minutes, cooled on ice for 5 minutes, and then centrifuged at high speed for 15 minutes. After centrifugation, 200 µl of the supernatant is transferred to a fresh tube, and 75 µl of 10% ammonium hydroxide is added to neutralize the acidity. Following neutralization, 150 µl of the sample is distributed into each well of a 96-well plate. The amount of calcium deposition is quantified by measuring the optical density at 405 nm using an ELISA reader (Alqutub *et al*., 2022).

Statistical Analysis

The data are collected, verified, adjusted, and organized in tables and figures using Microsoft Excel 2016. Outlier detection and management are carried out using IBM-SPSS version 29.0. Normality testing is conducted to assess the distribution of data, distinguishing between parametric and nonparametric distributions. The Shapiro-Wilk test is utilized for this purpose at a significance level of 0.05. Parametric data are summarized in terms of the means ± standard deviation (SD). A one-way analysis of variance (ANOVA) is performed to compare the means of multiple treatment groups using inferential statistics, with the ANOVA significance threshold set at $p \le 0.05$. Post-hoc analysis using the Bonferroni test is employed for pairwise comparisons when a significant result is obtained from the ANOVA. The physical and mechanical studies involve six samples (n = 6) and triplicates (n = 3) for cell culture testing in the pre-experimental group. Statistical analyses are conducted using the SPSS software (IBM-SPSS ver. 29.0 for Mac OS) (Knapp, 2017).

RESULTS

Characterization of the eggshell powder

The composition and chemical analysis of the eggshell powder are presented in Table (1), in which CaO and other mineral oxide were proved. The table provides a comprehensive breakdown of the oxide mineral concentrations in the eggshell sample, highlighting the presence of various elements such as calcium oxide (CaO), magnesium oxide (MgO), sodium oxide (Na_2O), potassium oxide (K_2O), iron oxide (Fe_2O_3), strontium oxide (SrO_2), silicon dioxide

(SiO$_2$), and phosphorus pentoxide (P$_2$O$_5$). The Loss on Ignition (LOI) percentage measured by Thermal Gravimetric Analysis (TGA) indicates the volatile content in the sample. This detailed analysis offers valuable insights into the composition of the material, aiding in further understanding its properties and potential applications. X-ray diffraction (XRD) analysis (Fig. 3) reveals a predominant phase of calcium carbonate with a composition of 96.10%, translating to 53.81% calcium oxide (CaO) as quantified via inductively coupled plasma mass spectrometry (ICP-MS). Subsequently, scanning electron microscopy (SEM) provided insights into the surface morphology of the eggshell powder, corroborated by energy-dispersive X-ray spectroscopy (EDX) analysis (Fig. 4). Thermal gravimetric analysis (TGA) demonstrated a weight loss of 45.44% upon heating to 1000°C. Furthermore, the thermal stability and fraction of volatile components were elucidated in Figure (5).

Characterization of the bioactivity of synthesized Bioglass powders in PBS

X-ray Diffraction (XRD)

The XRD analysis of both the Nano-bio-glass (B.G.) ceramic powders demonstrates the presence of amorphous state phases with a hollow hump between 2θ = 20 and 30 (Figs. 6, A and B). XRD patterns of both powders reveal the formation of the hydroxyapatite HAp) phase (Figs. 6, A and B) after 14 days of incu-

bation in PBS. BG derived from eggshells reveals a higher relative intensity of the HAp phase than that derived from pure chemicals.

Attenuated Total Reflection Fourier Transform Infrared (ATR-FTIR)

The spectra of bioglass (BG) powders are given in Figs. (7) and (8) before and after soaking in PBS. Before immersion, the BG powders exhibit absorption bands at approximately 797–99 and 472-70 cm^{-1}. These bands correspond to the symmetric stretching and bending vibrations of the silicon-oxygen-silicon (Si-O-Si) bonds in the framework structure of the bioglass (Jayalekshmi *et al.*, 2013).

Upon soaking in PBS, new absorption bands are observed at approximately 613–09 and 592-61 cm^{-1}. These bands are attributed to the triply degenerated modes ν 4a and ν 4c of the oxygen-phosphorus-oxygen (O-P-O) bonds in the phosphate group (PO$_4$)$^{3-}$ of the hydroxyapatite (HAp) mineral phase (Gheisari *et al.*, 2015).

SEM and EDX micrographs

An aggregate of irregular, globular-shaped particles of bioglass with different crystal sizes is observed by SEM (Figs. 10(A) and 11(B). They display the Kα radiation of Ca, Si, Na, O, and P. Both bioglass powders showed Kα radiation of the C element. Furthermore, the SEM images reveal that hydroxyapatite crystals start to form on the surface of

Table (1): Compositional analysis of oxide minerals and loss on ignition (LOI) percentage in eggshell powder sample (calcined at 1000°C).

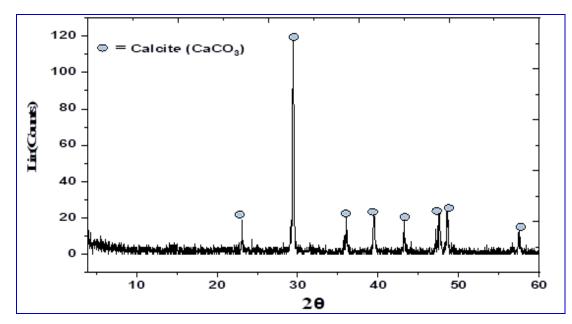| Concentration (Wt. %)	Identified oxide minerals								LOI (%) (as measured by TGA)
	CaO	MgO	Na$_2$O	K$_2$O	Fe$_2$O$_3$	SrO$_2$	SiO$_2$	P$_2$O$_5$	
	50.98	0.71	0.59	0.61	0.45	0.08	0.47	0.63	45.44

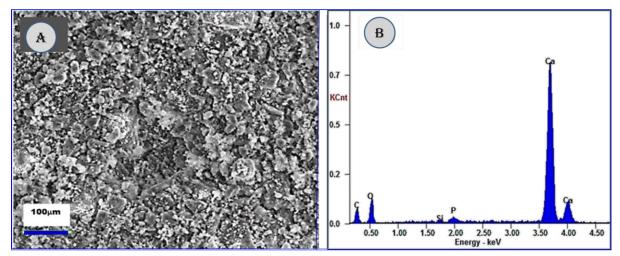**Figure (3):** XRD Pattern of Raw Eggshell powder

Figure (4): Characterization of eggshell powder. A, Scanning electron microscopy (SEM) delivered the surface morphology of the eggshell powder; B, Energy-dispersive X-ray spectroscopy (EDX) analysis.
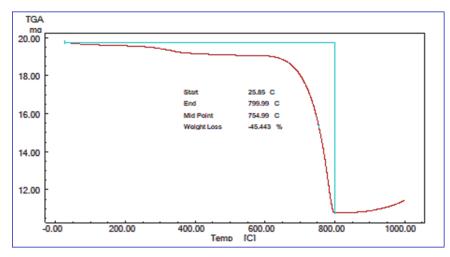

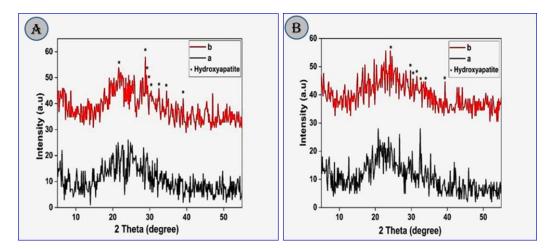**Figure (5):** Thermal Gravimetric Analysis (TGA) point out the volatile content in the eggshell powder.

Figure (6): X-ray diffraction (XRD) patterns of BG prepared from pure chemicals (A) in comparison to NBG prepared from biogenic eggshells (B). Balck line (a) and Red line (b) refers to the measurement before and after soaking in PBS for 14-days, respectively.

7

Figure (7): FTIR spectra of the NBG synthesized chemically before (A) and after (B) soaking in PBS for 14 days (The arrow indicates the formation of new HAp crystals)
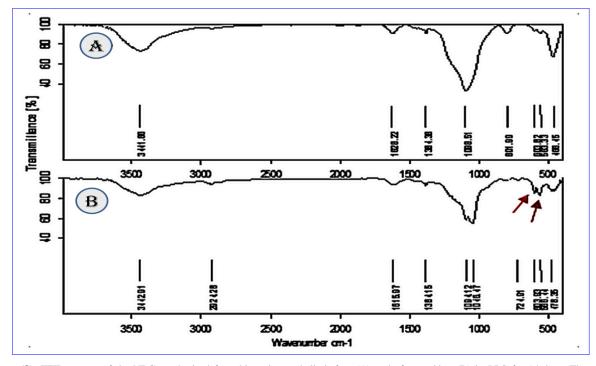

Figure (8): FTIR spectra of the NBG synthesized from biogenic eggshells before (A) and after soaking (B) in PBS for 14-days (The arrow indicates the formation of new HAp crystals)

8

the original ceramic powders, as shown in Figures (9B and 10B). These hydroxyapatite crystals are more abundant in specimens derived from biogenic sources.

Transmittance Electron Microscopy (TEM) of bioglass powders

The transmission electron microscopy (TEM) micrographs reveal that both types of bioglass display spheroidal, partially agglomerated nanostructures. The average particle size observed for the chemically synthesized BG is 16 nm, while the eggshell-derived BG exhibits an average particle size of 14 nm. These findings are depicted in Figure (11).

Physico-mechanical characterization of the scaffolds
Porosity

SEM images depict a highly porous structure with well-defined, interconnected open pores ranging in size from 325 to 440 μm. For group I, group II and group III, the average pore size recorded 440 , 334 and 325 μm, respectively (Fig. 12). The scaffold-free BG (group I) possesses the largest mean pore sizes and smoother pore walls compared to the other composite scaffolds, in addition to a uniform thickness and homogeneous spatial distribution of pores. Although the scaffolds containing BG (II and III) do not show a relatively large difference between their average pore sizes, they show higher interconnectivity than group I

scaffolds. Many BG particles exist inside the internal walls of the pores consolidating them with an apparent decrease in the number of open pores. Moreover, SEM analysis suggests an accum-ulation of the ceramic particles being deeply embedded in the porous PCL/Zein matrix.

The mean porosity for various scaffolds (Figure 13) reveals a statistically significant difference in porosity (%) across groups ($p \leq 0.001$). PCL/Zein scaff-olds (group I) have the highest value (81.33%). Adding bioglass (chemically synthesized and from eggshells) to the PCL/Zein matrix (groups II and III) decreased the porosity percentage to 73%.

Mechanical strength (Compressive strength: MPa)

The compressive strength results (Figure 14) showed that PCL/Zein scaffolds (group I) have the lowest value (2.9 MPa). Adding synthetic bioglass to the PCL/Zein matrix (groups II) shows a statistically significant increase in compressive strength value (4.5 MPa) while adding bioglass from eggshells shows a slight, nons-ignificant increase (3.6 MPa) compared to group I ($p \leq 0.015$).

Biodegradation (weight loss %)

The incorporation of bioglass, as filler in the PCL/Zein matrix, significantly enhances the weight loss percentage, as observed in Figure (15), increasing
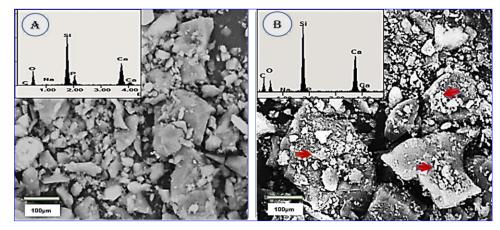
Figure (9): SEM and EDX images of the aggregated NBG particles synthesized from pure chemicals before (A) and after (B) 14 days of soaking in PBS. The arrow indicates the formation of hydroxyapatite crystals on the surface of the bioglass. Bar, 100 μm
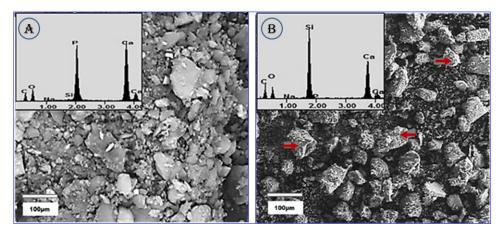
Figure (10): SEM and EDX images of the aggregated NBG particles synthesized from biogenic eggshells before (A) and after (B) 14 days of soaking in PBS. The arrow indicates the formation of hydroxyapatite crystals on the surface of the bioglass. Bar, 100 μm.
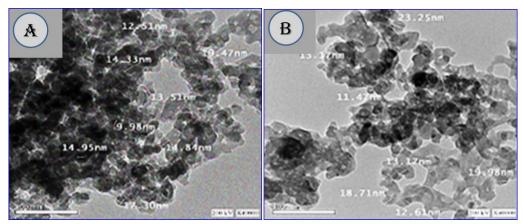
Figure (11): TEM images and particle size dimensions of NBG: Chemically synthesized (A) and biogenic egg - shell derived (B).

from 16.56% to 28.7% in group I and group II, respectively. However, in group III the increment was up to 30.58% with statistically significant differences ($p \leq 0.001$). Imaging of scaffold group (III) with PCL, Zein, and BG (biogenic eggshells) before and after six months of degradation in PBS at 37 ± 1 $^{\circ}$C (Fig. 16) showed degradation from the scaffold outside edges and a broken-down internal structural framework.

The scaffold's in vitro bioactivity

SEM and EDX

SEM results show the formation of irregular crystals of hydroxyapatite after immersion in PBS for 14 days (Fig. 17). These crystals are found on both the surface and internal walls of the porous composite scaffolds. Sample III with the biogenic BG type shows the most surface coverage with the residue and the highest Ca and P K_{α} radiation intensities. The existence of Kα radiation of Ca, Si, O, Na, and P elements in scaffold groups II and III is due to the existence of bioglass. The appearance of K_{α} radiation from Na and Cl elements arises from the immersion solution (PBS). The presence of Kα radiation of the nitrogen (N) element in all scaffold groups arises from the zein protein structure, while K_{α} radiation of carbon (C) is due to the presence of (CH_2) n-chains in the PCL polymer structure as well as amino acids in the zein protein structure.

Thermal Analysis and Evaluation (DTA and T.G.) of the scaffolds

The thermal analysis (DTA/TG) of scaffold groups (I) and (III) is shown in Fig. (18). Scaffold group (I) shows three endothermic peaks at 67, 366, and 403°C, respectively, while group (III), containing biogenic bioglass, only reveals two endothermic bands at 67 and 410°C. While T.G. curves show three different stages of scaffold degradation, group (I) showed a faster rate of thermal degradation than Group (III).

Biological characterization

Viability % test

The cell viability (%) of several groups tested at different time intervals showed a statistically insignificant increase in cell viability (%) values with time. Furthermore, statistically insignificant differences exist in viability (%) mean values between the different groups. A representative SE microscopy of biogenic BG scaffold group III represents the morphology of the MSCs developed on the scaffold after seven days (Figure 19). The scanning electron microscopy (SEM) image reveals globular-shaped cells with flat and extending expansions of cells (Figure 20).

Alkaline phosphatase (ALP) absorbance at 405 nm (Osteogenic differentiation)

The results (Figure 21) show a statistically significant increase in ALP absorbance with time for all groups (p-value <0.001). There is no significant variation in ALP absorbance between the different groups on days 1 and 7 (p-values = 0.420 and 0.473, respectively). On day 3, the scaffolds containing bioglass from different sources (groups II and III) revealed statistically significantly higher values compared with group I (p-value =0.003).

Alizarin Red Test for Mineralization Assessment

The average calcium absorbance levels recorded at various time intervals (3, 7, and 15 days) indicate a progressive increase in absorbance from day 3 to day 15, with the peak mean values observed for each group on day 15 (Fig. 22). On days 3 and 7, scaffolds that contain bioglass from eggshells show the highest absorbance value compared with the other groups. On day 15, scaffolds that contain bioglass from different sources as filler in their matrix show a statistically significant increase in mean calcium absorbance values compared with group I, with no statistically significant difference in Ca absorbance values between groups II and III. Figure (23) shows the photomicrograph of the alizarin red staining of calcium deposits on different scaffolds after 15 days.

DISCUSSION

Composite scaffolds have great potential as materials for bone tissue regeneration. By integrating polymers with bioceramics, the advantageous properties of polymer flexibility and malleability, as well as the enhanced strength, rigidity, and bioactivity of bioceramic
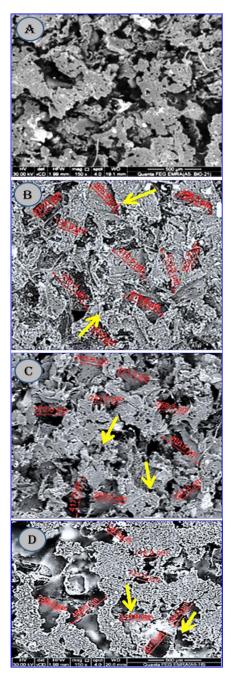
Figure (12): SEM images show a highly porous structure with well-defined, interconnected open pores ranging in size from 325 to 440 μm. A, scaffold before immersion in PBS for 14 days; B, C, and D represent three different scaffold groups after immersion in PBS for 14 days. Bar, 500 μm.

Figure (13): Porosity (%) in different scaffold groups.

Figure (14): Compressive strength in different scaffold groups.

Figure (15): Weight loss in different scaffold groups.

are synergistically harnessed to produce scaffolds with enhanced mechanical and biological capab-ilities. Polycaprolactone and zein protein polymers are currently of interest due to their biocompatibility, good mechanical properties, and availability. Among the most promising bio ceramic materials are calc-ium phosphates (such as hydroxyapatite, biphasic HAp/β-TCP, and bioglass), which can either be chemically prepared or extracted from biogenic sources, owing to their natural affinity and tendency to bond directly to bone tissues (Dutta *et al*., 2011).

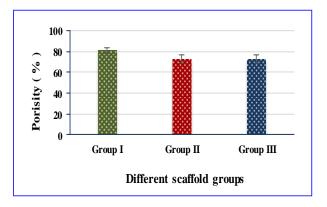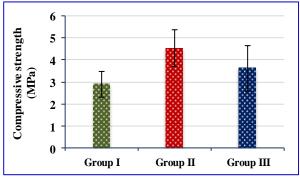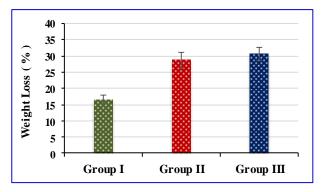In the present study, eggshells are used as a valuable source of CaO in the synthesis of bioglass using a sol-gel route. Since eggshells are a rich source of calcium carbonate ($CaCO_3$), exceeding 94%, they can also be used as a calcium oxide (CaO) precursor for the synthesis of calcium phosphate biomaterials. It also contains some trace metal ions, such as Mg^{2+}, Si^{4+}, P^{5+}, Na^+, etc., which may enhance the bioactivity of the bioglass by promoting cell adhesion, stability, and stimulating bone formation. Because eggshells are normally abundant in nature and are often discarded, their different applications might reduce environmental pollution. Also, the use of eggshells as a source of CaO allows low-cost bioglass production since the content of calcium oxide (CaO) represents about 46% of the total bioglass weight (Palakurthy *et al*., 2020). About 96% of calcium carbonate is reported in our results after being calculated on the basis of calcium oxide (CaO) following calcination of the raw eggshells at 1000 °C. Other researchers have found that the carbonate content of heat-untreated eggshells is approx
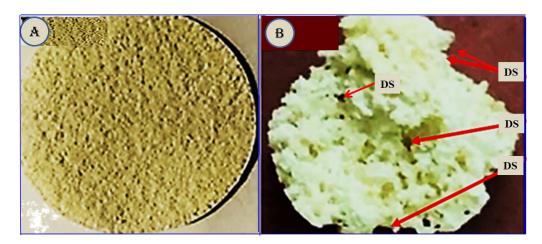
11

Figure 16: The extent of polymeric scaffold degradation contained NBG eggshells derived (group-III). A, shows the scaffold before immersion in PBS; B, shows the scaffold after immersion in PBS for 6 months. Arrows pointed to degraded scaffold. DS, degraded sites.
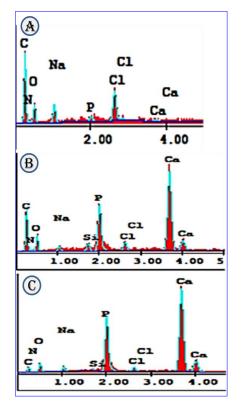

Figure (17): Dispersive X-ray Spectroscopy (EDX) Analysis of the scaffold after immersion in PBS for 14 days showed different mineral constituents of hydroxyapatite formed.

imately 94% (Azis et $al.$, 2018; Ma et $al.$, 2023). This difference may be due to the volatilization of organic matter at high temperatures.

Two different types of nanosized bio-glass powders are produced, having the same chemical composition ($CaO-SiO_2-Na_2O-P_2O_5$ = 46.1-26.9-34.4-2.6 mole %) but of different precursors. The first is made from pure chemical reagents, while the second is made from calcined eggshells as a source of CaO. Both types of B.G. that are prepared by sol-gel routes and calcined at 700°C show a higher dissolution rate and bioactivity C show a higher dissolution rate and bioactivity compared to the melt-cast material of the same chemical composition (Radandima et $al.$, 2021).

The data from XRD, FTIR, SEM, EDX, and TEM of bio-glasses characterization confirm the absence of any secondary phase in both types of B.G. powders. The EDX analysis data (Figs. 10A and 11A) proved the presence of Kα radiation for Ca, Si, Na, and P elements. Unreal values of carbon content are detected in both types of B.G. Strong Kα radiation of carbon elements in the B.G. solids are detected. It may be attributed to the carbon tabs (carbon double phase) on which the samples are mounted (aluminum folder) in the EDX instrument. Furthermore, upon the existence of environmental carbon dioxide (CO_2) in the presence of water during the synthesis, carbonates can form on the bioglass surface (Perardi et $al.$, 2005).
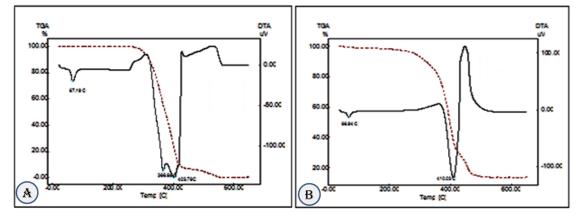

Figure (18): Differential thermal analysis (DTA) of PCL/Zein scaffolds (A) and PCL/Zein/NBG scaffolds (B).
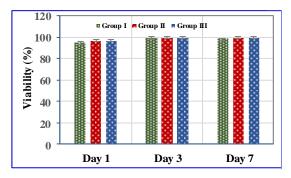
Figure (19): Viability percent of scaffolds of the three groups at different time intervals 1, 2 and 3 days.
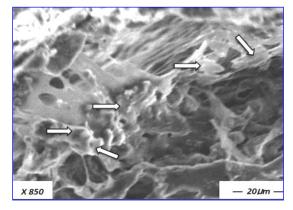

Figure (20): SE micrograph of cellular growth on the composite scaffold contained NBG-eggshells derived (group-III) which indicate cell viability. Bar, 20 μm.
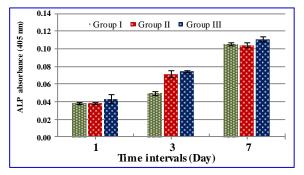

Figure (21): Alkaline phosphatase (ALP) Absorbance (mean ±SE) in various groups of scaffold at different time intervals.
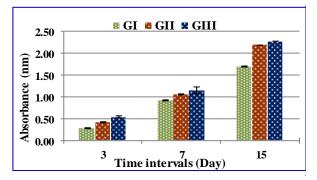

Figure (22): Calcium Absorbance (mean ±SE) in various groups of scaffold at different time interivals.

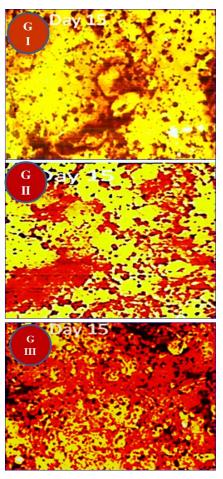The TEM of the B.G. powders (Figure 11) reveals agglomeration of Nano spheroidal crystallites (16 and

Figure (23): Photomicrograph, of alizarin red staining of calcium deposits on scaffolds after 15 Days, showing a progressive increase in absorbance along different tested groups.

14 nm in diameter) for chemically synthesized and eggshell-derived, respectively. Based on the results obtained, it is expected that these BG materials are highly bioactive, reacting faster due to their high surface areas achieved by decreasing their particle sizes to the Nano scale. The bone-bonding ability of the synthesized bioglass powders is commonly evaluated through their ability to form an apatite layer on their surface when immersed in PBS (Loh *et al.*, 2023; Varila *et al.*, 2012). This apatite layer binds the B.G. surface to the apatite bone and interacts with the collagen fibrils of damaged bone fibrils (Jones, 2015).

After immersion in PBS, the bioglass ceramic powders show some changes in the spectra of XRD, FTIR, and EDX. The XRD results (Fig. 6 A and B) show the appearance of relatively strong diffraction peaks in both types of B.G. samples around $2\theta = 31.80$ (dÅ = 2.80), corresponding to the reflection of a newly formed hydroxyapatite phase (Hong *et al.*, 2009). The reflection peak is higher in eggshell-derived BG compared to the pure chemically synthesized one. This confirms the ability of BG powders to induce the formation of apatite layers on their surfaces. Despite the close difference in particle size (14-16 nm) between the two types, eggshell-derived BG is still more active than the other. This may be attributed to the presence of some minor metal ions in the eggshells (Table 1).

FTIR spectroscopy (Figs. 7 and 8) confirms the formation of an apatite layer via a split P-O band peak (604 and 564 cm^{-1}) for the chemically synthesized B.G. and the eggshell-derived B.G. powder (603 and 566 cm^{-1}), as well as those assigned to the bending of O-P modes of hydroxyapatite vibrations (Jayalekshmi *et al.*, 2013). Moreover, the symmetric stretching vibration of ν (Si-O-Si) at 797 cm^{-1} for both B.G. types and the asymmetric stretching vibration of Si-O-Si and P-O-P (1105 and 1103 cm^{-1}) shift to frequencies (799 cm^{-1}) and (1102 and 1100 cm^{-1}) after 14 days of immersion in PBS for the chemically synthesized and eggshell B.G. powders, respectively. The bands located at 1102 and 1100 cm^{-1} become more intense, indicating an interaction between the bioglass framework and PBS solution, finally helping the deposition of HAp layers on the B.G. surface (Chatzistavrou *et al.*, 2006; Hong *et al.*, 2009).

After immersion in PBS solution, according to SEM results (Figs. 9 and 10), a new aggregate crystal fully covers the BG crystal surfaces. Additionally, EDX shows an increase in the Kα radiation intensities of Ca, P, and C, confirming the presence of a new carbonated apatite layer from beta-type (β-HCA) (Gavinho *et al.*, 2022), which is also consistent with the FTIR results. EDX results also confirm the decrease in intensity of Si K_α compared to the unsoaked B.G. powder. In this respect, the soluble Si^{4+} ions from the B.G. could serve as a heterogeneous nucleation site to induce apatite formation in the solution, which confirms the bioactivity of the B.G. The formation of silica-induced apatite coincides with the silica-induced precipitation of calcium phosphate, where the release of Si^{4+} and Ca^{2+} ions from B.G. powder into the SBF medium and an exchange with H$^+$ in the SBF might be associated with an increased pH value of the medium (Gavinho *et al.*, 2022; Nandi *et al.*, 2016).

The advantageous use of nanoparticles rather than micro particles in the composite scaffolds for higher bioactivity with optimized mechanical strength is noticed. This phenomenon arises from the gradual release of Si^{4+} and Ca^{2+} ions from the bioglass structure, which stimulates the osteoblasts involved in cell signalling at the genetic level. Furthermore, the development rate of the hydroxyapatite (HCA) layer on the surface of bioactive glass (B.G.) is affected by the pace at which B.G. degrades and the presence of Na$_2$O, which enhances the rate of HAp layer formation (Hajiali *et al.*, 2018).

The enhanced biological activity of the eggshell composition (Table 1) can be attributed to the presence of more active ions. The findings of our investigation align with the findings of a recent study conducted by Srinath *et al.* (2020) and Palakurthy *et al.* (2020). They successfully synthesize SiO$_2$–CaO–Na$_2$O bioactive glass using a melt-quenching method. In their work, they utilize bio-waste materials such as silica rice husk ash (RHA) and eggshells as precursors for SiO$_2$ and CaO. This glass exhibits significant bioactivity, as seen by the rapid formation of the hydroxyapatite (HAp) layer on its surface within seven days of being incubated in simulated body fluid (SBF). Furthermore, the cytocompatibility data demonstrate that it has no harmful effects on MG-63 cells at different concentrations (ranging from 50 to 1000 μg/ml) after two days of culture.

Solvent casting is one of the techniques used for composite scaffold fabrication. This method is fast, cheaper, different diameters of pore sizes are formed, and it is easy to remove NaCl salt from the polymeric scaffold. It is capable of producing scaffolds with an interconnected pore structure that is controlled by pore size and distribution (Thadavirul *et al.*, 2014). After dissolving the polymer in a suitable organic solvent, it is mixed with a porogen (NaCl). NaCl is used as a porogen in this work as it remains the gold standard due to its ease of use, very low price, and high solubility, which ensures complete porogen removal.

It is evident from electron microscope images of the synthesized scaffolds (Fig. 12) that they have an interconnected, highly porous structure with pore sizes of 325–440 μm (Table 2). The pores have a distinct interior cubic structure, like that of the NaCl porogen particles. The diversity in pore sizes and diameters facilitates the attachment and proliferation of cells, as well as new tissue ingrowth and vascularization. It has also been reported that macro porous scaffolds (100 and 600 μm) allow better integration, vascularization, permeability, and bone distribution with the host bone tissue, increasing the growth of the bone. However, small pores are more appropriate for the growth of soft tissue (Abbasi *et al.*, 2020).

The Nano-bioglass adds to the PCL/zein scaffold matrix, causing some changes in both the micro-structure and morphology of the fabricated composite scaffolds (Fig. 12). Evidently, the pore walls of the bioglass-free scaffold (group I) exhibit a smoother texture compared to the pore walls of the other composite scaffolds. The incorporation of B.G. ceramic powder into the PCL/zein matrix results in a reduction in the average pore size. This could be attributed to the agglomerated clusters formed by the BG fillers added around and inside the pores. Another parameter that may affect the average pore sizes is the percentage of the grain sizes of the NaCl porogen (250 to 500 μm), possibly varying from batch to batch. The addition of inorganic fillers such as HAp and BG to the PCL matrix can occupy the free pore space, thereby reducing its dimensions (Fanovich *et al.*, 2023). This suggestion agrees with our results, as the nano-bioceramics are readily accessible following the full dissolution (extraction) of the NaCl porogen, resulting in rough pore walls of the PCL/zein bio ceramic scaffolds (as seen in the scanning electron micrographs of scaffold groups II and III). Such rough surfaces in scaffolds would act as favorable sites for the osteoblast's attachment, promoting faster tissue ingrowth (Zuo *et al.*, 2021). Since they are highly porous, the microstructures of the fabricated composite scaffolds in the present study are expected to be highly promising, with a well-developed network of interconnected pores with sizes exceeding a hundred

microns. These findings agree with the porosity data calculated statistically in this study (Fig.13). The statistical results reveal a satisfactory high percent of porosity in the prepared composite scaffolds, in a range of about 73-82 percent. Group I show a higher porosity percentage (81.33%) compared to the lower porosity percentages of groups II and III (73%).

In general, smaller pore sizes, gradient porosity, and staggered-oriented pores are correlated with a higher compressive module of the synthesized scaffolds (Hajiali *et al.*, 2018). The statistical analysis of the study reveals a notable rise in the compressive strength from 2.90 MPa in group I to 4.53 MPa in group II. However, there was no significant difference between groups I and III or between groups II and III, as shown in Figure (14). The enhanced compressive strength values are a result of the inclusion of B.G. in the PCL/zein polymer matrix, which serves as rigid filler and enhances both the stiffness and compressive strength of the composite scaffolds (Daskalakis *et al.*, 2022). The enhanced mechanical characteristics resulting from these fillers can be attributed to the reduced porosity and pore dimensions. The compressive strength values of the scaffold groups examined (Fig. 14) fall within the range of cancellous bone (2–12 MPa) (Muthutantri *et al.*, 2010), suggesting that they are appropriate for use in bone tissue engineering applications in places that do not sustain loads.

The degradation process of the PCL polymer typically spans 3-4 years, rendering it a favored option for extended implantation and bone tissue engineering applications. PCL has excellent solubility in commonly used organic solvents. Its capacity to create polymer-polymer blends enables convenient mixing of PCL with polymers that degrade more rapidly, hence enhancing both mechanical properties and degradation rate (Hajiali *et al.*, 2018).

Biodegradation of polymeric scaffolds may guide and regulate the proliferation and activities of supported cells. It is known that PCL polymers are highly hydrophobic, and it takes 2-3 years for complete degradation. In our results, it lost about 30% of its original weight after 180 days. In this study, due to the hydrolytic degradation after six months of immersion in PBS, the weight loss (%) ranges from 16.53 to 30.58% (Fig. 15). An addition of Nano-bioglass powder to PCL/zein scaffold matrices improves the degradation rate. Introducing 20% of the bioglass ceramic powders, chemically synthesized and synthesized from eggshells, enhances the degradation rate from 16.53% (Group I) to 28.72% (Group II) and 30.58% (Group III). The statistical analysis reveals a noteworthy disparity between group I and the remaining groups while indicating a statistically inconsequential distinction between groups II and III. The results are consistent with previously published data (Mao *et al.*, 2018), indicating the enhanced breakdown of PCL scaffolds when B.G. is added in vitro. During the initial period of degradation, these fillers enhance the water absorption (hydrophilicity) of the scaffolds (Mao *et al.*, 2018).

The enhanced rate of deterioration of the PCL/Zein scaffold can also be attributed to the confinement of ceramic fillers inside the PCL/Zein matrix, which hinders the production of PCL crystallites in the composite blend. The reduced crystallinity of the composite scaffolds leads to an accelerated chemical hydrolysis rate as the ester linkage in the amorphous phase becomes more easily accessible. The inclusion of ceramic fillers leads to the formation of a polymer/ceramic interface that is prone to hydrolytic degradation (Woodard & Grunlan, 2018). Also, it has been found that the inclusion of zein protein polymers into the PCL matrix increases its hydrophilicity by reducing the water contact angle with water and hence increasing the PCL degradation rate (Wu *et al.*, 2012).

The study conducted by Fereshteh *et al.* (Fereshteh *et al.*, 2016) shows that the degradation rate of PCL is influenced by the PCL: Zein ratio in composite scaffolds. Specifically, an elevated quantity of zein in the scaffolds leads to an enhanced degradation rate of PCL. This possible formation of a hydrogen bond between PCL and Zein polymers enhances their water accessibility, thus making them more hydrophilic. In the present study, it is found that there is an increase in scaffold group III degradation rate compared to group II. This may be attributed to the presence of some cations, such as Mg^{2+}, Si^{4+}, Sr^{2+}, P^{5+}, etc., associated with eggshell structure. These cations can coordinate with water, which leads to improving the hydrophobicity of the scaffolds and raising the rate of degradation. The presence of surface roughness, with numerous small fissures and tiny pores, in the degraded scaffold (III) (Fig. 16) enhances the interconnectivity.

Scaffolds containing biogenic bioglass (III) reveal higher thermal stability than bioglass-free scaffolds (I). The BG particles (group III) can act as a barrier that hinders the diffusion of heat and prevents thermal degradation of the polymer matrix. Additionally, minor amounts of metal ions, such as Mg^{2+}, Si^{4+}, P^{5+}, etc., can be bonded with the polymer matrix (PCL/Zein) of the scaffold during the synthesis process. These bonds strengthen the interfacial interactions between the bioglass particles and the polymer matrix, leading to improved overall thermal stability.

To evaluate the efficiency of the biomaterials on the living bones, the formation of carbonated apatite layers on the implant surface is required. Dispersed new apatite crystals with different crystal sizes on the surfaces and inside the inner walls of scaffolds are detected in SEM (Fig. 17). Their density is the highest in scaffolds containing biogenic BG (group III), which may be due to the presence of silicon ions (Si^{4+}) and some other minor metal ions in their composition (Obata *et al.*, 2022). This result is consistent with an increase in the concentration values of both K_α radiations for Ca and P elements measured by the EDX technique after immersion in PBS for 14 days (Fig.17C). Additionally, the presence of B.G. in an amorphous state makes the surface area larger,

resulting in a higher rate of dissolution and faster formation of carbonated hydroxyapatite layers on the scaffold's surface.

Mesenchymal stem cells (MSCs) are used for in vitro biological activity in cell-based tests. Regeneration of bone treatments relies on various factors, such as the use of cells, biomaterials, and others. Many benefits of cell transplantation with MSCs exist since these multipotent cells are both capable of migrating to locations of damage and suppressing the local immune response (Qin *et al*., 2014). In the present study, bone marrow MSCs derived from the rat's femur are seeded onto the synthetic porous composite scaffolds due to their unique properties of having a significant potential for multiline age differentiation, attachment, and growth, in addition to being easily accessible and culturally expandable, with outstanding genomic stability (Kim *et al*., 2019).

The viability of r-MSC cultivated on the composite scaffolds is assessed using the MTT test at time intervals of 1, 3, and 7 days. This method is a straightforward quantitative colorimetric technique that relies on the reduction of a yellow tetrazolium salt (MTT) to generate purple formazan crystals by metabolically active cells. In this study, there is a slight enhancement in cell viability of the scaffolds containing biogenic glass (group III) compared to the chemically synthesized bio-glass due to the presence of some minor metal ions, such as Si^{4+}, Sr^{2+}, Mg^{2+}, P^{5+}, etc., associated with the eggshell's composition. Trace elements play a crucial role in bone regeneration and expedite the process of bone production (Firdaus Hussin *et al*., 2022; Mohd Pu'ad *et al*., 2019). Hengzhang Lin *et al*. (Lin *et al*., 2021) show that a concentration of 4-10 mM of inorganic phosphorus (P) might increase hBM–MSC migration, osteogenic differentiation, and mineralization. The statistical viability percentage data of the different scaffold groups for incubation periods of 1, 3, and 7 days was statistically insignificant (Fig. 19). The scaffolds show a viability range of about 95-99%. The number of viable cells increases with increasing incubation time in the groups containing bioglass. The high surface area of BG provides more sites for protein adsorption and growth factors, improving cell attachment and proliferation.

Additionally, the release of Si^{4+} ions during its dissolution enhances osteoblastic proliferation and activity (Axrap *et al*., 2016; Obata *et al*., 2017). On the other hand, BG has a hydrophilic nature, which reduces the intrinsic hydrophobicity of PCL and zein proteins and enhances their interaction with cells (Ilyas *et al*., 2022). The differentiation and activity of r-MSC on the synthesized scaffolds were examined by evaluating the ALP absorbance at 1, 3, and 7 days of culture. The results (Fig. 21) indicate a statistically significant change in ALP absorbance by time within each tested scaffold group, which increases with increasing culture time. The mean absorbance values of ALP after seven days are statistically significantly higher than values on days 1 and 3. However, on day 7, there are no statistically significant differences between the different groups. The Zein protein demonstrates excellent biocompatibility with human endothelial vein cells (HUVECs), human liver cells (HL-7702), rat mesenchymal stem cells, and mouse fibroblast cells (NIH 3T3), indicating its potential as a polymer material for bone tissue engineering applications (Demir *et al*., 2017). The L929 cell culture conducted on Zein scaffolds demonstrates cell adhesion and growth, with a cell survival of over 90% after three days, thereby showing the biocompatible nature of the scaffolds. The incorporation of Zein protein into poly (ε-caprolactone) 3D scaffolds is seen to enhance the cytoaffinity of NIH/3T3 mouse embryonic fibroblasts and H1299 human lung cancer cells (Jing *et al*., 2018). These results agree with scaffold group I, which contains PCL/Zein after seven days of culture.

The optical microscopic images of ARS-stained composite scaffolds detect slight reddish dots on their surfaces on day 3. The color intensity of the reddish dots appears to be higher in samples II and III. The color intensity of the orange-red dots increases on day 7. At day 15, the ARS in all scaffolds shows increased color intensity, with the highest intensities in scaffold groups II and III (Figs. 22 and 23). This implies the time dependence of cell mineralization to produce Ca^{2+} ion binding sites for ARS, also showing the effectiveness of B.G. ceramic for cell mineralization (Mozafari & Moztarzadeh, 2014). A significant statistical difference is seen in the Ca^{2+} absorbance values with time across the various groups (P-value < 0.001). Based on statistical analysis, there is a considerable rise in the average absorbance from day 3 to day 7, as well as from day 7 to day 15. The scaffold groups II and III always reveal the highest values in calcium absorbance, suggesting higher mineralization and higher activity of the cells. Thus, these scaffolds may be considered to have promising potential for bone tissue engineering regeneration (Mozafari & Moztarzadeh, 2014).

CONCLUSION

Highly pure and active nano-sized bioglass can be synthesized from biogenic eggshells at a low production cost, offering a sustainable solution to reduce environmental pollution. This bioglass ceramic exhibits promising bioactivity by forming a carbonated hydroxyapatite layer upon immersion in phosphate-buffered saline (PBS). Incorporating bioglass ceramics derived from eggshells into PCL scaffold matrices enhances their biodegradation rate, mechanical properties, thermal stability, and bioactivity. Among the tested groups, Group III, containing eggshell-derived bioglass, demonstrates the highest bioactivity attributed to the presence of minor ions (e.g., Mg^{2+}, P^{5+}, Sr^{2+}, Si^{4+}) inherent in the eggshell structure, which promote cellular bioactivity. SEM analyses reveal that the solvent casting/particulate leaching method yields composite scaffolds with a highly porous, interconnected structure and average pore diameters ranging

from 325 to 440 µm, making them conducive to supporting bone tissue formation. The compressive strength values of the scaffold groups align with the mechanical strength of cancellous bone (2-12 MPa), indicating their suitability for bone tissue engineering applications. Furthermore, the study proposes the potential application of biogenic bioglass in dentistry for developing oral care products due to its enhanced bioactivity compared to pure sol-gel chemical synthesis methods.

REFERENCES

ABBASI N, HAMLET S, LOVE RM, NGUYEN NT. 2020. Pours scaffolds for bone regeneration: J.Sci.: Adv. Mater.Devices,; 5(1):1-9.

ALQUTUB M. N., MUKHTAR A. H., ALALI Y., VOHRA F., & ABDULJABBAR T. 2022. Osteogenic Differentiation of Periodontal Ligament Stem Cells Seeded on Equine-Derived Xenograft in Osteogenic Growth Media. Medicina 58(11):1518.

AXRAP A., WANG J., LIU Y., WANG M., & YUSUF A. 2016. Study on adhesion proliferation and differentiation of osteoblasts promoted by new absorbable bioactive glass injection in vitro. European Review for Medical and Pharmacological Sciences 20(22):4677-4681.

AZIS Y., ADRIAN M., ALFARISI C. D., KHAIRAT, & SRI R. M. 2018. Synthesis of hydroxyapatite nanoparticles from eggshells by sol-gel method. IOP Conference Series: Materials Science and Engineering 345:012040.

CHATZISTAVROU X., ZORBA T., CHRISSAFIS K., KAIMAKAMIS G., KONTONASAKI E., KOIDIS P., & PARASKEVOPOULOS K. M. 2006. Influence of particle size on the crystallization process and the bioactive behavior of a bioactive glass system. Journal of Thermal Analysis and Calorimetry 85(2):253-259.

DASKALAKIS E., HUANG B., VYAS C., ACAR A. A., FALLAH A., COOPER G., WEIGHTMAN A., KOC B., BLUNN G., & BARTOLO P. 2022. Novel 3D Bioglass Scaffolds for Bone Tissue Regeneration. Polymers 14(3):445.

DEMIR M., RAMOS-RIVERA L., SILVA R., NAZHAT S. N., & BOCCACCINI A. R. 2017. Zein-based composites in biomedical applications. Journal of Biomedical Materials Research Part A 105(6):1656-1665.

DIBA M., FATHI M. H., & KHARAZIHA M. 2011. Novel forsterite/polycaprolactone nanocomposite scaffold for tissue engineering applications. Materials Letters 65(12):1931-1934.

DUTTA A., FERMANI S., ARJUN TEKALUR S., VANDERBERG A., & FALINI G. 2011. Calcium phosphate scaffold from biogenic calcium carbonate by fast ambient condition reactions. Journal of Crystal Growth 336(1):50-55.

FANOVICH M. A., DI MAIO E., & SALERNO A. 2023. Current Trend and New Opportunities for Multifunctional Bio-Scaffold Fabrication via High-Pressure Foaming. Journal of Functional Biomaterials 14(9):480.

FERESHTEH Z., FATHI M., BAGRI A., & BOCCACCINI A. R. 2016. Preparation and characterization of aligned porous PCL/zein scaffolds as drug delivery systems via improved unidirectional freeze-drying method. Materials Science and Engineering: C 68:613-622.

FIRDAUS HUSSIN M. S., ABDULLAH H. Z., IDRIS M. I., & ABDUL WAHAP M. A. 2022. Extraction of natural hydroxyapatite for biomedical applications-A review. Heliyon 8(8):e10356.

GAUTAM S., SHARMA C., PUROHIT S. D., SINGH H., DINDA A. K., POTDAR P. D., CHOU C.-F., & MISHRA N. C. 2021. Gelatin-polycaprolactone-nanohydroxyapatite electrospun nanocomposite scaffold for bone tissue engineering. Materials Science and Engineering: C 119:111588.

GAVINHO S. R., PÁDUA A. S., SÁ-NOGUEIRA I., SILVA J. C., BORGES J. P., COSTA L. C., & GRAÇA M. P. F. 2022. Biocompatibility, Bioactivity, and Antibacterial Behaviour of Cerium-Containing Bioglass®. Nanomaterials 12(24):4479.

GENG Z., CHENG Y., MA L., LI Z., CUI Z., ZHU S., LIANG Y., LIU Y., BAO H., LI X., & YANG X. 2018. Nanosized strontium substituted hydroxyapatite prepared from egg shell for enhanced biological properties. Journal of Biomaterials Applications 32(7):896-905.

GHEISARI H., KARAMIAN E., & ABDELLAHI M. 2015. A novel hydroxyapatite - Hardystonite nanocomposite ceramic. Ceramics International 41(4):5967-5975.

HAJIALI F., TAJBAKHSH S., & SHOJAEI A. 2018. Fabrication and Properties of Polycaprolactone Composites Containing Calcium Phosphate-Based Ceramics and Bioactive Glasses in Bone Tissue Engineering: A Review. Polymer Reviews 58(1):164-207.

HAMZA E. H., TEMRAZ T. A., & AHMED S. A. 2015. Bioactivity of Some Egyptian Seaweeds Extract. CATRINA 11(1).

HONG Z., REIS R. L., & MANO J. F. 2009. Preparation and in vitro characterization of novel bioactive glass ceramic nanoparticles. Journal of Biomedical Materials Research Part A 88A(2):304-313.

ILYAS K., AKHTAR M. A., AMMAR E. BEN, & BOCCACCINI A. R. 2022. Surface Modification of 3D-Printed PCL/BG Composite Scaffolds via Mussel-Inspired Polydopamine and Effective Antibacterial Coatings for Biomedical Applications. Materials 15(23):8289.

JAYALEKSHMI A. C., VICTOR S. P., & SHARMA C. P. 2013. Magnetic and degradable polymer/bioactive glass composite nanoparticles for biomedical applications. Colloids and Surfaces B: Biointerfaces 101:196-204.

JING L., WANG X., LIU H., LU Y., BIAN J., SUN J., & HUANG D. 2018. Zein Increases the Cytoaffinity and Biodegradability of Scaffolds 3D-Printed with Zein and Poly(ε-caprolactone) Com-

posite Ink. ACS Applied Materials & Interfaces 10(22):18551-18559.

JONES J. R. 2015. Reprint of: Review of bioactive glass: From Hench to hybrids. Acta Biomaterialia 23: S53-S82.

KIM H., BAE C., KOOK Y.-M., KOH W.-G., LEE K., & PARK M. H. 2019. Mesenchymal stem cell 3D encapsulation technologies for biomimetic micro-environment in tissue regeneration. Stem Cell Research & Therapy 10(1): 51.

KNAPP H. 2017. Introductory Statistics Using SPSS. SAGE Publications, Inc.

LIN H., ZHOU Y., LEI Q., LIN D., CHEN J. & WU C. 2021. Effect of inorganic phosphate on migra-tion and osteogenic differentiation of bone marrow mes-enchymal stem cells. BMC Develop.Biol.21(1): 1.

LOH Z. W., MOHD ZAID M. H., AWANG KECHIK M. M., FEN Y. W., AMIN K. M., & CHEONG W. M. 2023. New formulation calcium-based 45S5 bioactive glass: In vitro assessment in PBS solution for potential dental applications. Journal of Materials Research and Technology 24: 3815-3825.

MA Q., RUBENIS K., SIGURJÓNSSON Ó. E., HILD-EBRAND T., STANDAL T., ZEMJANE S., LOCS J., LOCA D., & HAUGEN H. J. 2023. Eggshell-derived amorphous calcium phosphate: Synthesis, characterization and bio-functions as bone graft materials in novel 3D osteoblastic spheroids model. Smart Materials in Medicine 4: 522-537.

MAO D., LI Q., LI D., TAN Y., & CHE Q. 2018. 3D porous poly(ε-caprolactone)/58S bioactive glass–sodium alginate/gelatin hybrid scaffolds prepared by a modified melt molding method for bone tissue engineering. Materials & Design 160: 1-8.

MOHD PU'AD N. A., KOSHY P., ABDULLAH H. Z, IDRIS M. I. & LEE T. C. 2019. Syntheses of hydr-oxyapatite from natural sources. Heliyon 5(5): e01588.

MOZAFARI M., & MOZTARZADEH F. 2014. Synth-esis, characterization and biocompatibility evalua-tion of sol-gel derived bioactive glass scaffolds prepared by freeze casting method. Ceramics Inter-national 40(4): 5349-5355.

MUTHUTANTRI A. I., EDIRISINGHE M. J., & BO-CCACCINI A. R. 2010. Improvement of the micr-ostructure and mechanical properties of bioceramic scaffolds using electrohydrodynamic spraying with template modification. Journal of the Mechanical Behavior of Biomedical Materials 3(3): 230-239.

Nandi, Samit Kumar, Arnab Mahato, Biswanath Kundu, and Prasenjit Mukherjee. 2016. 'Doped Bioactive Glass Materials in Bone Regeneration'. Advanced Techniques in Bone Regeneration. InTech. doi:10.5772/63266.

OBATA A., IWANAGA N., TERADA A., JELL G., & KASUGA T. 2017. Osteoblast-like cell responses to silicate ions released from 45S5-type bioactive glass and siloxane-doped vaterite. Journal of Materials Science 52(15): 8942-8956.

OBATA A., LEE S., & KASUGA T. 2022. Bioactive glass materials for tissue regeneration. Journal of the Ceramic Society of Japan 130(8): 22054.

PALAKURTHY S., REDDY K. V., PATEL S., & AZ-EEM P. A. 2020. A cost effective SiO_2-CaO-Na_2O bio-glass derived from bio-waste resources for biomedical applications. Progress in Biomaterials 9(4): 239-248.

PERARDI A., CERRUTI M., & MORTERRA C. 2005. Carbonate formation on sol-gel bioactive glass 58S and on Bioglass® 45S5. Stud. Surface Sci. & Catalysis 461-469.

PÉREZ-GUZMÁN C. J., & CASTRO-MUÑOZ R. 2020. A Review of Zein as a Potential Biopolymer for Tissue Engineering and Nanotechnological App-lications. Processes 8(11):1376.

QI J., YU T., HU B., WU H., & OUYANG H. 2021. Current Biomaterial-Based Bone Tissue Engin-eering and Translational Medicine. International Journal of Molecular Sciences 22(19):10233.

QIN Y., GUAN J., & ZHANG C. 2014. Mesenchymal stem cells: mechanisms and role in bone regenera-tion. Postgraduate Medical J. 90(10-69):643-647.

RADANDIMA A., AROFAH S. K., AMALIA H. A. R., & NURBAITI U. 2021. Review: nanocomposite of bioactive glass/forsterite from raw material sand and egg shell for bone and dental implants. Journal of Physics: Conference Series 1918(2):022018.

SANGEETHA P, MAITI SK, DIVYA M, SHIV-ARAJU S, RAGUVARAN R, MALIK R, BIND-HUJA BV, NAVEEN KUMAR, RAGUVANSHI PDS, 2017. Techniques for isolation, expansion and differentiation. Stem Cell Res Ther. 3(3):10-1.

THADAVIRUL N., PAVASANT P., & SUPAPHOL P. 2014. Improvement of dual-leached polyca-prolactone porous scaffolds by incorporating with hydroxyapatite for bone tissue regeneration. Journal of Biomaterials Science, Polymer Edition 25(17):-1986-2008.

VARILA L., FAGERLUND S., LEHTONEN T., TU-OMINEN J., & HUPA L. 2012. Surface reactions of bioactive glasses in buffered solutions Journal of the European Ceramic Society 32(11):2757-2763.

WOODARD L. N., & GRUNLAN M. A. 2018. Hyd-rolytic Degradation and Erosion of Polyester Biom-aterials. ACS Macro Letters 7(8):976-982.

WU F., WEI J., LIU C., O'NEILL B.& NGOTHAI Y. 2012. Fabrication and properties of porous scaffold of zein/PCL biocomposite for bone tissue engin-eering. Composites Part B: Eng. 43(5):21-92-2197.

XIA W., & CHANG J. 2007. Preparation and charac-terization of nano-bioactive-glasses (NBG) by a quick alkali-mediated sol-gel method. Mat-erials Letters 61(14–15):3251-3253.

ZHANG R., LI X., LIU Y., GAO X., ZHU T., & LU L. 2019. Acceleration of Bone Regeneration in Cri-tical-Size Defect Using BMP-9-Loaded nHA/ColI/-MWCNTs Scaffolds Seeded with Bone Marrow Mesenchymal Stem Cells. BioMed Research International 2019:1-10.

ZUO W., YU L., LIN J., YANG Y., & FEI Q. 2021. Prop-erties improvement of titanium alloys scaffolds in bone tissue engineering: a literature review. Annals of Translational Medicine 9(15):1259.

تقييم في المختبر للنشاط البيولوجي للزجاج الحيوي المشتق من قشر البيض الحيوي بحجم النانو – والبولي كابرولاكتون- وبروتين الذرة (الزين) لتصنيع، سقالات مركبة ثلاثية الأبعاد لهندسة الأنسجة العظمية

أماني صبري القرشي، ،'محمد سعيد الشهيدى[2]، رانيا السعدي بدوي[1] ، نور أحمد حبيب[3]

[1] قسم المواد الحيوية لطب الأسنان، كلية طب الأسنان، جامعة قناة السويس، الإسماعيلية

[2] قسم الفيروسات، كلية الطب البيطري، جامعة قناة السويس، الإسماعيلية

[3] قسم المواد الحيوية لطب الأسنان، كلية طب الأسنان، جامعة القاهرة

الملخص العربي

فى تلك الدراسة المختبرية ، تم تحضير سقالات نشطة بيولوجيا لتستخدم فى تطبيقات مجال هندسة الأنسجة العظمية كبديل للأنسجة التالفة فى الأنسان معتمدة على الزجاج الحيوى النانو والمستخلص من مخلفات قشور البيض والتى تعتبر من الملوثات البيئة و ذلك بطريقة الصول جل. تم مقارنة هذا النوع المنتج من الزجاج الحيوى بأخرمحضر كلية من مواد الكيميائية الخالصة . وتتكون تلك السقالات من بوليمرات البولى كابرولاكتون وبروتين الذرة (الزبين) والزجاج الحيوى. تم توصيف تلك السقالات من حيث المسامية وقوة التحمل الميكانيكى ودرجة الأنحلال البيولوجى، هذا بالأضافة الى النشاط البيولوجى لها وذلك بذرع خلايا جزعية عليها مستخلصة من الجرزان . وأثبتت الدراسة أن الزجاج الحيوى المستخلص من المخلفات البيولوجية كانت أكثر كفاءة للسقالات من الناحية البيولوجية . وبناء على ذلك توصى تلك الدراسة بأمكانية تحضير وتصنيع الزجاج الحيوى من مخلفات قشور البيض والمستخدم فى تحضير السقالات والأنسجة العظمية كبديل للأنسجة التالفة. هذا بالأضافة الى امكانية أستخدام هذا الزجاج الحيوى فى مواد داعمة فى مجال طب الأسنان**.**